

Analysis of Microstrip Lines using Vector Dyadic Green's Function

N. Gupta

*Department of Electronics & Communication Engineering, Birla Institute of Technology
Mesra, Ranchi- 835 215, India*

D.K. Gupta

*Department of Mathematics, Indian Institute of Technology
Kharagpur-721302, India, e-mail: dkg@maths.iitkgp.ernet.in*

Introduction

The analysis of guided wave structures constitutes a major part of the microwave engineering. Several numerical techniques have been used in the past to analyze the transmission lines such as microstrip, slot, coplanar lines. The Spectral domain method was the most preferred methods in the past. Specially, when one deals with mutli-layered structures or structures with conductors at several interfaces, the Spectral Domain immittance approach based on coordinate transformation is preferred the most. The formulation of Green's function may be done almost by inspection in many structures. On the whole, the Spectral domain method is known to be efficient but is restricted in general to the well-shaped structures. On the other hand, a semi analytical method involving discretization such as the Method of Lines (MOL), can be applied to a number of practical but analytically complex structures. In addition, unlike the Spectral domain method, it does not require any basis function. Both the methods, however formulate the eigenvalue problems thus deriving the Green's matrix, which relates the current densities on the strip to the field.

The equivalence between the Spectral Domain Approach (SDA) and the Method of Lines (MOL) [1]-[3] show that the basic difference between the two lies with the fact that in case of SDA each element of the Green's matrix is a scalar but in the case of the MOL it is a vector. In other words, MOL is a discrete form of SDA. Deriving the Green's function in SDA is always an easy task especially when Immitance approach [4] and [5] is being used. The spectral domain Green's functions can be readily derived in the closed form for most of the microstrip/fin line configurations and using the equivalence criteria the MOL solution can directly be derived from the SDA formulation by simple manipulation. The motivation of the present study is to show that the equivalence criteria can be utilized to derive the Vectorized Green's function directly from the Green's function in SDA. The Green's function so derived are then used to determine the dispersion and current distribution on the transmission line. In this case, the same basic formulations can be used for both the purposes.

In the present paper, the Vectorized Green's functions are first derived from the spectral domain Green's function and then utilized to compute the dispersion characteristics and the current distribution of the microstrip lines in simple and suspended configurations. The analysis is presented for triple layers of dielectric substrates. Finally, the dispersion characteristics are compared with the SDA result. A very good agreement between the two results is obtained.

The paper has been organized as follows: Section 2 discusses the formulation of the problem using the equivalence criteria. Section 3 presents the numerical results and finally section 4 gives the conclusion.

Formulation

For a two dimensional transmission line problem of the type shown in Fig.1, the wave equation can be written as

$$\frac{\partial^2 \varphi^{e,h}}{\partial x^2} + \frac{\partial^2 \varphi^{e,h}}{\partial y^2} - (k^2 - \beta^2) \varphi^{e,h} = 0 \quad (1)$$

with $k^2 = \omega^2 \mu_0 \epsilon_0 \epsilon_r$. φ^e and φ^h are the electric and magnetic scalar potentials and, β is the propagation constant along z. The SDA involves the Fourier transformation while MOL deals with the discretization as shown in Fig.1. In both SDA and MOL, the transformation is performed along the (direction to convert a partial differential equation to a normal one dimensional differential equation and for each MOL and SDA it is represented as:

$$\varphi \Rightarrow \bar{\varphi}, \quad \bar{\varphi} \Rightarrow \hat{\varphi}, \quad \hat{\varphi} = [T]\varphi, \quad (2)$$

$$\varphi \Rightarrow \hat{\varphi}, \quad \hat{\varphi} = \int_{-\infty}^{+\infty} \varphi e^{j\alpha_n x} dx, \quad (3)$$

where, $[T]$ is the orthogonal transformation matrix and α_n is the spectral term as in [7] and [8].

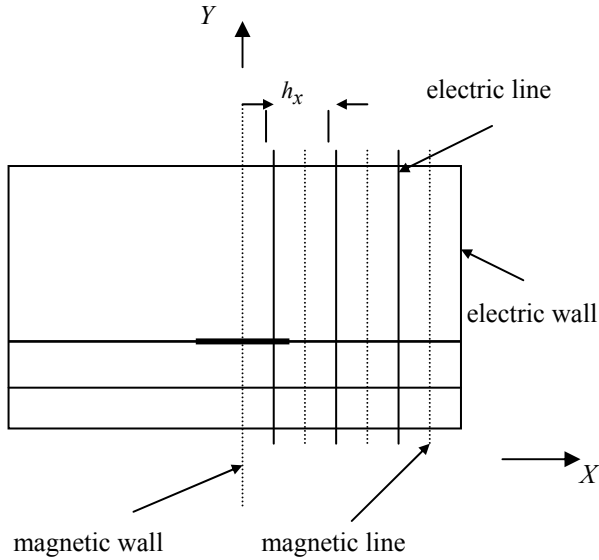


Fig. 1. Enclosed microstrip configuration on a two-layer dielectric substrate showing discretization in half space

This shows that the orthogonal transformation in MOL is equivalent to discrete Fourier transform in SDA. Following these equivalence criteria the spectral domain Green's functions can be readily transformed to the Vectorized Green's functions, which relates the field to the current density functions. In vector form of the Green's matrix, each element of the Green's function matrix is a sub matrix. Assuming the harmonic time dependence $\exp(j\omega t)$ and the propagation behavior in the z-direction according to $\exp(-j\omega t)$ the scalar potentials φ^e and φ^h must satisfy the Helmholtz equation given in (1). Performing the discretization along x in MOL, equation (1) takes the form as

$$\frac{d^2}{dy^2} \tilde{\varphi}_{e,h} - \left(\frac{[Q_{e,h}]}{h_x^2} - (k^2 - \beta^2)[I] \right) [\tilde{\varphi}_{e,h}] = [0], \quad (4)$$

where, $[Q_e]$ and $[Q_h]$ are the symmetrical tridiagonal matrices respectively written as

$$[Q_e] = -[D_e][D_h], \quad (5)$$

$$[Q_h] = -[D_h][D_e], \quad (6)$$

where $[D_e], [D_h]$ - the bidiagonal matrices as given in [6]. To obtain an explicit solution of the discretized equation, one needs to implement certain transformation procedure namely the orthogonal transformation. $[Q_e]$ and $[Q_h]$ can be transformed into the diagonal form as:

$$[T_{e,h}]^{-1} [Q_{e,h}] [T_{e,h}] = [\lambda_{e,h}] = [\delta][\delta^t], \quad (7)$$

where, $[\lambda_e], [\lambda_h]$ - the diagonal eigenvalue matrices of $[Q_e]$ and $[Q_h]$. $[T_e]$ and $[T_h]$ are the corresponding eigenvector matrices of $[Q_e]$ and $[Q_h]$.

For a symmetrical structure, $[\lambda_e]$ and $[\lambda_h]$ are the

same and equal to $[\delta]^2$. Similarly, $[\varphi^e]$ and $[\varphi^h]$ can be transformed to $[\tilde{\varphi}^e]$ and $[\tilde{\varphi}^h]$ as

$$[\varphi_{e,h}] = [T_{e,h}][\tilde{\varphi}_{e,h}]. \quad (8)$$

After orthogonal transformation, equation (4) takes the form as:

$$\frac{d^2}{dy^2} \tilde{\varphi}_{e,h} - \left(\frac{[\delta^2]}{h_x^2} - (k^2 - \beta^2)[I] \right) \tilde{\varphi}_{e,h} = [0] \quad (9)$$

However in SDA equation (1) takes the form as:

$$\frac{d^2}{dy^2} \hat{\varphi}_{e,h} - (\alpha_n^2 - (k^2 - \beta^2)) \hat{\varphi}_{e,h} = [0]. \quad (10)$$

Comparing the above two equations it is clearly evident that the equation (9) is nothing but a vectorized form of the equation (10), where the spectral term α_n a scalar, is replaced by the term $[\delta]^2 / h_x^2$, the vector eigen values. Similar transformation is also obvious in the field equations for each of the dielectric regions.

After suitable transformation, each element of the dyadic spectral Green's function matrix in vectorized form is written as,

$$[\tilde{G}_{zz}] = [\tilde{G}_1], \quad (11)$$

$$[\tilde{G}_{zx}] = [\tilde{G}_2], \quad (12)$$

$$[\tilde{G}_{xz}] = [\tilde{G}_2], \quad (13)$$

$$[\tilde{G}_{xx}] = [\tilde{G}_1], \quad (14)$$

where

$$[\tilde{G}_1] = [-\tilde{Y}_1]([\tilde{Z}_2][\tilde{Z}_e] + [\tilde{Z}_1][\tilde{Z}_h]), \quad (15)$$

$$[\tilde{G}_2] = [-\tilde{Y}_2]([\tilde{Z}_e] - [\tilde{Z}_h]), \quad (16)$$

$$[\tilde{G}_3] = [-\tilde{Y}_1]([\tilde{Z}_1][\tilde{Z}_e] + [\tilde{Z}_2][\tilde{Z}_h]), \quad (17)$$

$$\tilde{Z}_1 = [\delta]^2 / h_x^2, \quad (18)$$

$$\tilde{Z}_2 = \beta^2, \quad (19)$$

$$\tilde{Y}_1 = 1/(\tilde{Z}_1 + \tilde{Z}_2), \quad (20)$$

$$\tilde{Y}_2 = (\beta[\delta]/h_x)/(\tilde{Z}_1 + \tilde{Z}_2). \quad (21)$$

$[\tilde{Z}_e]$ and $[\tilde{Z}_h]$ can be obtained as follows for a three layer substrate:

$$[\tilde{Z}_e] = \left([\tilde{T}_7]^{-1} + [\tilde{T}_5]^{-1} \right), \quad (22)$$

$$[\tilde{Z}_h] = \left([\tilde{T}_8]^{-1} + [\tilde{T}_6]^{-1} \right), \quad (23)$$

$$[\tilde{T}_1] = [\tilde{A}_3][\tilde{X}_3]^{-1}, \quad (24)$$

$$[\tilde{T}_2] = [\tilde{X}_3][\tilde{B}_3]^{-1}, \quad (25)$$

$$[\tilde{T}_3] = [\tilde{A}_2]([\tilde{A}_3][\tilde{X}_2] + [\tilde{A}_2][\tilde{X}_3]),$$

$$([\tilde{A}_2][\tilde{X}_2][\tilde{X}_3]+[\tilde{A}_3])^{-1}, \quad (26)$$

$$[\tilde{T}_4]=[\tilde{B}_2]^{-1}([\tilde{B}_2][\tilde{X}_2]+[\tilde{B}_3][\tilde{X}_3]),$$

$$([\tilde{B}_3][\tilde{X}_2][\tilde{X}_3]+[\tilde{B}_2])^{-1}, \quad (27)$$

$$[\tilde{T}_5]=[\tilde{A}_1]([\tilde{T}_3][\tilde{X}_1]+[\tilde{A}_1]),$$

$$([\tilde{A}_1][\tilde{X}_1][\tilde{T}_3])^{-1}, \quad (28)$$

$$[\tilde{T}_6]=[\tilde{B}_1]^{-1}([\tilde{B}_1][\tilde{T}_4][\tilde{X}_1]),$$

$$([\tilde{X}_1]+[\tilde{B}_1][\tilde{T}_4]), \quad (29)$$

$$[\tilde{T}_7]=[\tilde{A}_0][\tilde{X}_0]^{-1}, \quad (30)$$

$$[\tilde{T}_8]=([\tilde{B}_0][\tilde{X}_0])^{-1}, \quad (31)$$

$$[\tilde{X}_i]=[\cot[\gamma_i]h_i], \quad i=1,2,3,4, \quad (32)$$

$h_2 = d, h_3 = h_2, h_4 = h_3$ and h_l are as defined in Fig. 2(c):

$$[\tilde{A}_i]=[\gamma_i]j\omega\epsilon_0\epsilon_r[I]^{-1}, \quad (33)$$

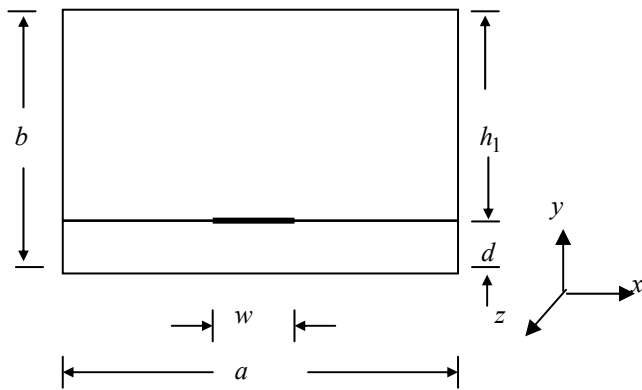
$$[\tilde{B}_i]=j\omega\mu[\gamma_i], \quad (34)$$

$$[\gamma_i]=\sqrt{\frac{[\delta]^2}{h_x^2}-(k^2-\beta^2)[I]}, \quad (35)$$

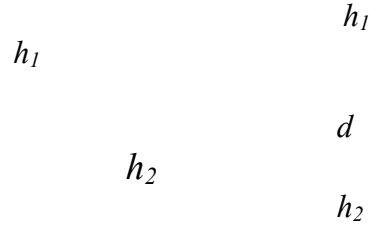
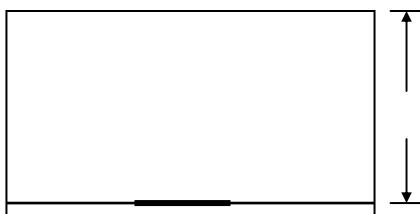
$$k^2=\omega^2\mu\epsilon_0\epsilon_r. \quad (36)$$

For a symmetrical structure along y as shown in Fig. 1, only half of the structure is considered and the matrix of eigen values, $[\delta]$, and the corresponding matrices of eigen vectors $[T_e]$ and $[T_h]$ are given as in [6].

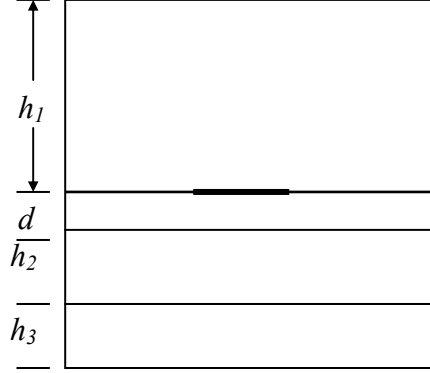
A close examinations of the above equations reveal that the only difference between the Spectral domain Green's function and the Green's function in MOL is that in the Spectral domain case, derivative with respect to x is replaced by the spectral term while in the case of the MOL they are replaced by the matrix obtained from the finite difference approximations of the derivatives.



(a) Simple microstrip line



(b) Suspended microstrip line



(c) Three layer microstrip line

Fig. 2. Various microstrip configurations

The above space-coupled Green's function needs to be back transformed so as to apply the final boundary conditions. This is done with the help of the orthogonal transformation matrices, i.e., the matrix of the eigen vectors. A detailed explanation is given in [6], [7], [8] and, [9]. The final matrix equation relating the current densities on the strip to the field is written as:

$$\begin{bmatrix} \tilde{e}_x \\ \tilde{e}_z \end{bmatrix} = \begin{bmatrix} [T_e][\tilde{G}_{zz}][T_e] & [T_e][\tilde{G}_{zx}][T_h] \\ [T_h][\tilde{G}_{xz}][T_e] & [T_h][\tilde{G}_{xx}][T_h] \end{bmatrix} \begin{bmatrix} \tilde{J}_x \\ \tilde{J}_z \end{bmatrix}. \quad (37)$$

Next, only small number of discretization lines passing through the strip are considered as the current is nonzero only on the strip. The reduced matrix equation is obtained as,

$$\begin{bmatrix} 0 \\ 0 \end{bmatrix}_{red} = \begin{bmatrix} [G_{zz}] & [G_{zx}] \\ [G_{xz}] & [G_{xx}] \end{bmatrix}_{red} \begin{bmatrix} J_x \\ J_z \end{bmatrix}_{red}. \quad (38)$$

The final matrix equation is solved for the zero of the determinant, which is a measure of the propagation parameter. Finally, substituting for the value of the propagation parameter, the unknown current densities on the strip is determined.

Results and discussion

In this section, dispersion curve and the current distribution are plotted for various microstrip configurations as shown in Fig. 2(a), (b), and (c). A comparison is also made between them with the SDA results. For a symmetrical structure along y , only half of the space is considered.

At first, the convergence of the method is examined with respect to N (the number of discretization lines in half space), for NE (number of electric lines passing through half of the strip) = 2,3,4,5,6,7,8,9. In Fig. 3, the convergence curves for the normalized E.d.c (Effective dielectric constants) are plotted as a function of N . The convergence unto second decimal places can be achieved even with a small number of lines as low as $N = 37$ for the strip width w equal to the dielectric thickness, and the value of ϵ_r as 2.2, 3.27 and 9.8.

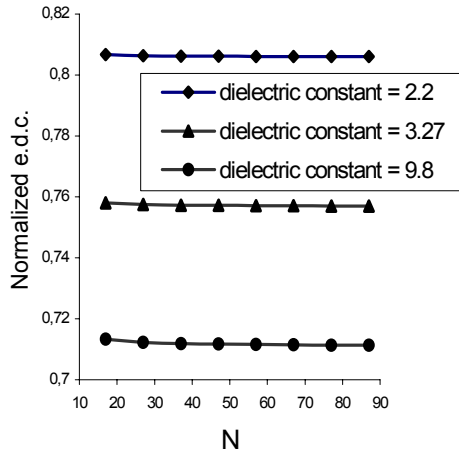


Fig. 3. Testing for the convergence of the method for single layer microstrip configuration, N - number of lines in half space, NE - number of e-lines passing through half of the strip = 2,3,4,5,6,7,8,9, dimension of the enclosure $a = b = 10w$, $w/d = 1$

The convergence is slower for the higher value of the ϵ_r , such as 9.8 compared to the other values 2.2 and 3.27. This is expected, since in the case of smaller value of the dielectric constant the fringing field is not as concentrated as for the case of higher dielectric constant and hence the convergence is fast. The difference between the effective dielectric constant for discretization lines, $N = 67$ and $N = 77$ is only 0.057 % for the $\epsilon_r = 9.8$. However, for clear representation of the current distribution on the strip, sufficient number of lines passing through the strip region is considered. Therefore, a figure of $N = 77$ is chosen so as to provide convergence for all the three cases and to provide $NE = 8$. It should be noted that for a very small strip width as low as $1/10$ of the dielectric thickness, a value of N even larger than 77 may be required. After the convergence of the method is examined, the method is utilized to compute the dispersion and current distribution of the microstrip in various configurations. In the first configuration, a microstrip line on a single layer substrate is considered having substrate with dielectric constant as $\epsilon_r = 2.2$. The thickness d , of the dielectric is assumed to be equal to the width of the strip = 0.254 mm. and, the dimensions of the enclosures as $a = b = 10w$. The dispersion characteristics are then plotted as a function of the strip width to the dielectric thickness ratio for both simple and suspended microstrip configurations as shown in Fig. 2. For a two-layer substrate, a suspended microstrip line configuration is considered where the dielectric constant of the lowest substrate is assumed to be 1. The strip is assumed to be suspended at a height $h_1 = b/2$, i.e.

in the middle of the enclosure. The effective dielectric constant value increases for the simple microstrip line while it decreases for the suspended line when the ratio of the strip width to dielectric thickness is increased. The dispersion characteristic shows good agreement with the SDA result. It should be noted that all the SDA results are plotted for the number of basis functions equal to one for both the components of the current densities J_x and J_z along x . A comparison with SDA result depicts a deviation for smaller w/d ratio while a reasonable matching is obtained for higher w/d ratio. This is because of the fact that MOL fails to yield efficient and accurate solutions when very narrow strips are considered in which strong singularities require an extra fine discretization. However, a fine discretization in turn requires more number of lines, which leads to computer time intensive algorithms. Similarly, in the case of SDA, more number of basis functions is required on the strip to yield accurate result for larger strip widths.

Fig. 4 shows the dispersion characteristics of the microstrip line as a function of the strip width.

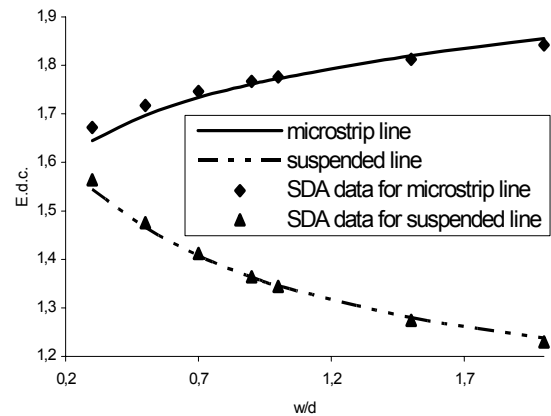


Fig. 4. Dispersion characteristics of various microstrip configurations as a function of strip width for $\epsilon_r = 2.2$ at $f = 30$ GHz., $a = b = 10w$

The value of the effective dielectric constant increases for the simple microstrip line while it decreases for the suspended line when the ratio of the strip width to the dielectric thickness is increased. A comparison with the SDA result shows a deviation for smaller w/d ratio while a reasonable matching is obtained for higher w/d ratio. This may be attributed to the fact that MOL fails to yield efficient and accurate solutions when the narrow strips are considered, where strong singularities require an extra fine discretization. However, a fine discretization in turn requires more number of lines which leads to computer-time intensive algorithms. Similarly, in the case of SDA, more number of basis functions are required on the strip to yield accurate result for larger strip widths. Fig. 5 shows the distribution of the current densities for simple, suspended and three layers substrate at 30 GHz. frequency.

For the three layer case, the dielectric constant of the lowest and the uppermost layers is assumed to be $\epsilon_r = 9.8$, and that of the middle layer is assumed to be 4.0. The thickness of each of the dielectric substrate is assumed to be $d = h_2 = h_3 = b/6$. As shown, the characteristic for the suspended line has the minimum current density

concentration at the two edges of the strip. Therefore, the area under the curve is minimum for this case, which signifies that it has the minimum current flow over the strip among all the three configurations and hence the minimum loss. The area under the curve increases for the higher dielectric constant values showing larger current concentration at the strip edges.

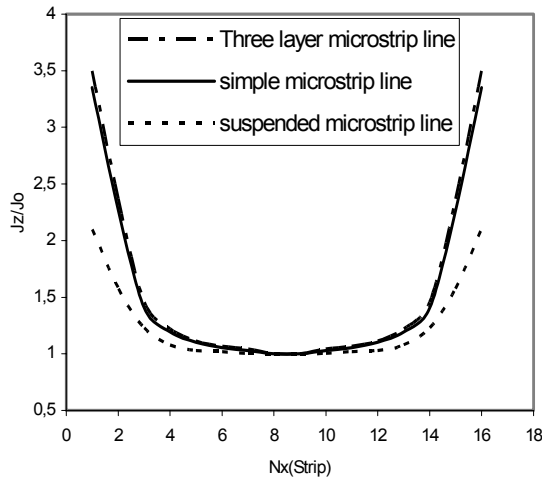


Fig. 5. Current distribution of various microstrip configurations at $f = 30$ GHz., $\epsilon_r = 2.2$, $a = b = 10w$, $w/d = 1$ and, $w = 0.254$ mm

Conclusion

An alternate approach has been presented thus deriving the Green's function in vector form (in MOL), directly from the Spectral domain Green's function (in SDA). The utility of the above approach lies with the fact that same set of equations can be used for the scalar and vector approach except that the scalar spectral domain Green's functions are Fourier transformed while in the vector form they are discretized. Similarly, the back transformation in SDA requires Galerkin's approach and in MOL they are back transformed using the matrices of the eigen vectors. This may

N. Gupta, D.K. Gupta. Mikrojuostelinių linijų analizė, įvertinant Gryno funkcijos dvimačių vektorių // Elektronika ir elektrotechnika. – Kaunas: Technologija, 2004. – Nr. 6(55). – P. 9-13.

Aprašoma bendroji teorija, kuri pagrįsta Gryno funkcijos dvimačiu vektoriumi. Apskaičiuota Gryno funkcijos tiesioginė priklausomybė, kai spektrinė analizė yra vertinama diskretinių sistemų lygtimis. Šis metodas gali būti pritaikytas planarinių mikrobanginių struktūrų bei rezonatorių analitiniams skaičiavimui. Siūloma šias lygtis taip pat vartoti mikrojuostelinių konfigūracijų charakteristikoms apskaičiuoti. Pateikiami mikrojuostelių pasiskirstymo konstrukcijų paviršiuose variantai. Gauti rezultatai sulyginimi su rezultatais, kurie gaunami naudojant spektrinius domenų. Il. 5, bib. 9 (anglų kalba; santraukos lietuvių, anglų ir rusų k.).

N. Gupta, D.K. Gupta. Analysis of Microstrip Lines using Vector Dyadic Green's Function // Electronics and Electrical Engineering. – Kaunas: Technologija, 2004. – No. 6(55). – P. 9-13.

This paper presents an approach to analyze the microstrip lines using Vector Dyadic Green's function. The vector Dyadic spectral Green's function is obtained directly from the Spectral domain immittance approach thus leading to a discretized system of equations which can be utilized in the semi analytical analysis of the planar microwave structures and resonators. Finally, the equations so derived have been used to analyze the characteristics of microstrip line in simple and suspended configurations. The current distribution on the strip is also calculated. The results thus obtained were found to be in good agreement with results using Spectral Domain Approach (SDA). Ill. 5, bibl. 9 (in English; summaries in Lithuanian, English and Russian).

Н. Гупта, Д.К. Гупта. Анализ микрополосковых устройств с использованием двумерных векторов функции Грина // Электроника и электротехника. – Каунас: Технология, 2004. – № 6(55). – С. 9-13.

Описывается общая теория анализа на основе двумерных векторов функции Грина. Установлена зависимость функции от разных соотношений векторов, когда спектральный анализ оценивается уравнениями дискретных функций. Предлагаемый метод рекомендуется использовать для планарных микрополосковых структур и аналитического расчета резонаторов. Приводится сравнение полученных результатов с результатами теории спектральных домен. Ил. 5, библи. 9 (на английском языке; рефераты на литовском, английском и русском яз.).

help in developing a Computer aided design software for the analysis various transmission lines, resonators and filters etc., while incorporating both the methods together.

References

1. **Gupta N., Singh M.** Space-spectral domain applied to a fin line configuration // IEEE Microwave and Guided wave Letters. – 1993. – Vol. 3, No. 3. – P. 125–126.
2. **Ming Yu, Vahldieck R., Wu Ke.** On the Nature and Application of the Space Spectral Domain Approach (SSDA) // IEEE Microwave Theory and Techniques Symposium Digest, 1994. - WE1B-333. - P. 591-594.
3. **Gupta N., Singh M.** Space-spectral domain analysis of rectangular fin line resonator // International Journal of Electronics. – 1996. – Vol. 81, No. 3. - P. 297-310.
4. **Itoh T.** Spectral domain immittance approach for dispersion characteristics of generalized printed transmission lines // IEEE Trans. Microwave Theory Tech. –1900. – Vol. MTT-28. – P. 733-736.
5. **Uwano T., Itoh T.** Spectral Domain Approach / in Itoh T. Ed. // Numerical Techniques for Microwave and Millimeter Wave Passive Structures. - New York: Wiley, 1989. – P. 335-380.
6. **Pregla R., Pascher W.** The method of Lines / in Itoh T. Ed. // Numerical Techniques for Microwave and Millimeter Wave Passive Structures. - New York: Wiley, 1989. - P. 381-446.
7. **Pascher W., Pregla R.** Full wave analysis of complex planar microwave structures // Radio Science. – 1987. - Vol. 22. - P. 999-1002.
8. **Schulz U., Pregla R.** A new technique for the analysis of the dispersion characteristics of planar waveguides and its application to microstrips with tuning septums // Radio Science. – 1981. - Vol. 16. - P. 1173-1178.
9. **Chen Z., Gao B.** Deterministic approach to full-wave analysis of discontinuities in MIC's using the method of lines // IEEE Trans. Microwave Theory Tech. – 1989. - Vol. 37. – P. 606-611.

Pateikta spaudai 2004 07 23